Robust and Efficient Generator of Almost Maximal Multipartite Entanglement

Davide Rossini[1,*] and Giuliano Benenti[2,3]

[1]NEST-CNR-INFM & Scuola Normale Superiore, Piazza dei Cavalieri 7, I-56126 Pisa, Italy
[2]CNISM, CNR-INFM & Center for Nonlinear and Complex systems, Università degli Studi dell'Insubria, via Valleggio 11, I-22100 Como, Italy
[3]Istituto Nazionale di Fisica Nucleare, Sezione di Milano, via Celoria 16, I-20133 Milano, Italy

(Received 3 July 2007; published 11 February 2008)

Quantum chaotic maps can efficiently generate pseudorandom states carrying almost maximal multipartite entanglement, as characterized by the probability distribution of bipartite entanglement between all possible bipartitions of the system. We show that such multipartite entanglement is robust, in the sense that, when realistic noise is considered, distillable entanglement of bipartitions remains almost maximal up to a noise strength that drops only polynomially with the number of qubits.

DOI: 10.1103/PhysRevLett.100.060501 PACS numbers: 03.67.Mn, 03.67.Lx, 05.45.Mt

Entanglement is not only the most intriguing feature of quantum mechanics but also a key resource in quantum information science [1,2]. In particular, for quantum algorithms operating on pure states, multipartite (many-qubit) entanglement is a necessary condition to achieve an exponential speedup over classical computation [3]. The entanglement content of random pure quantum states is almost maximal [4–6]; such states find applications in various quantum protocols, like superdense coding of quantum states [6,7], remote state preparation [8], and the construction of efficient data-hiding schemes [9]. Moreover, it has been argued that random evolutions may be used to characterize the main aspects of noise sources affecting a quantum processor [10].

The preparation of a random state or, equivalently, the implementation of a random unitary operator requires a number of elementary one- and two-qubit gates exponential in the number n_q of qubits, thus becoming rapidly unfeasible when increasing n_q. On the other hand, pseudorandom states approximating to the desired accuracy the entanglement properties of true random states may be generated efficiently, that is, polynomially in n_q [10–12]. In particular, quantum chaotic maps are efficient generators of multipartite entanglement among the qubits, close to that expected for random states [11,13]. A related crucial question is whether the generated entanglement is robust when taking into account unavoidable noise sources affecting a quantum computer that in general turn pure states into mixtures, with a corresponding loss of quantum coherence and entanglement content. In this Letter we give a positive answer to this question.

The number of measures needed to fully quantify multipartite entanglement grows exponentially with the number of qubits. Different measures capture various aspects of multipartite entanglement. Therefore, following Ref. [14], we characterize multipartite entanglement by means of a function rather than with a single measure: we look at the probability density function of bipartite entanglement between all possible bipartitions of the system. For pure states the bipartite entanglement is the von Neumann entropy of the reduced density matrix of one of the two subsystems: $E_{AB}(|\psi\rangle\langle\psi|) = -\mathrm{Tr}[\rho_A \log_2 \rho_A] \equiv S(\rho_A)$, where $\rho_A = \mathrm{Tr}_B(|\psi\rangle\langle\psi|)$, and A, B denote two subsystems made up of n_A and n_B qubits ($n_A + n_B = n_q$). For sufficiently large systems ($N \equiv 2^{n_q} \gg 1$), it is reasonable to consider only balanced bipartitions, i.e., with $n_A = n_B$, since the statistical weight of unbalanced ones becomes negligible [14]. If the probability density has a large mean value $\langle E_{AB}\rangle \sim n_q$ ($\langle\cdot\rangle$ denotes the average over balanced bipartitions) and small relative standard deviation $\sigma_{AB}/\langle E_{AB}\rangle \ll 1$, we can conclude that genuine multipartite entanglement is almost maximal (note that E_{AB} is bounded within the interval $[0, n_q]$). This is the case for random states [14].

The model.—The use of quantum chaos for efficient and robust generation of pseudorandom states carrying large multipartite entanglement is nicely illustrated by the example of the quantum sawtooth map [15]. This map is described by the unitary operator $\hat{U}$:

$$|\psi_{t+1}\rangle = \hat{U}|\psi_t\rangle = e^{-iT\hat{n}^2/2} e^{ik(\hat{\theta}-\pi)^2/2} |\psi_t\rangle, \qquad (1)$$

where $\hat{n} = -i\partial/\partial\theta$, $[\hat{\theta}, \hat{n}] = i$ (we set $\hbar = 1$) and the discrete time t measures the number of map iterations. In the following we will always study map (1) on the torus $0 \le \theta < 2\pi$, $-\pi \le p < \pi$, where $p = Tn$. With an n_q-qubit quantum computer we are able to simulate the quantum sawtooth map with $N = 2^{n_q}$ levels; as a consequence, θ takes N equidistant values in the interval $0 \le \theta < 2\pi$, while n ranges from $-N/2$ to $N/2 - 1$ (thus setting $T = 2\pi/N$). We are in the quantum chaos regime for map (1) when $K \equiv kT > 0$ or $K < -4$; in particular, in this work we focus on the case $K = 1.5$.

There exists an efficient quantum algorithm for simulating the quantum sawtooth map [15]. The crucial observation is that the operator $\hat{U}$ in Eq. (1) can be written as the product of two operators, $\hat{U}_k = e^{ik(\hat{\theta}-\pi)^2/2}$ and $\hat{U}_T = e^{-iT\hat{n}^2/2}$, that are diagonal in the θ and in the n representation, respectively. Therefore, the most convenient way to

classically simulate the map is based on the forward-backward fast Fourier transform between θ and n representations, and requires $O(N\log_2 N)$ operations per map iteration. On the other hand, quantum computation exploits its capacity to vastly parallelize the Fourier transform, thus requiring only $O((\log_2 N)^2)$ one- and two-qubit gates to accomplish the same task [15]. In brief, the resources required by the quantum computer to simulate the sawtooth map are only logarithmic in the system size N, thus admitting an exponential speedup, as compared to any known classical computation.

Multipartite entanglement generation.—We first compute $\langle E_{AB}\rangle$ as a function of the number t of iterations of map (1). Numerical data in Fig. 1 exhibit a fast convergence, within a few kicks, of this quantity to the value

$$\langle E_{AB}^{\mathrm{rand}}\rangle = \frac{n_q}{2} - \frac{1}{2\ln 2} \tag{2}$$

expected for a random state [4]. Precisely, $\langle E_{AB}\rangle$ converges exponentially fast to $\langle E_{AB}^{\mathrm{rand}}\rangle$, with the time scale for convergence $\propto n_q$ (see inset of Fig. 1). Therefore, the average entanglement content of a true random state is reached to a fixed accuracy within $O(n_q)$ map iterations, namely $O(n_q^3)$ quantum gates. We stress that in our case a deterministic map, instead of random one- and two-qubit gates as in Ref. [12], is implemented. Of course, since the overall Hilbert space is finite, the above exponential decay in a deterministic map is possible only up to a finite time and the maximal accuracy drops exponentially with the number of qubits. We also note that, due to the quantum chaos regime, properties of the generated pseudorandom state do not depend on initial conditions, whose characteristics may even be very different from it (e.g., in simulations of Fig. 1, we start from completely disentangled states).

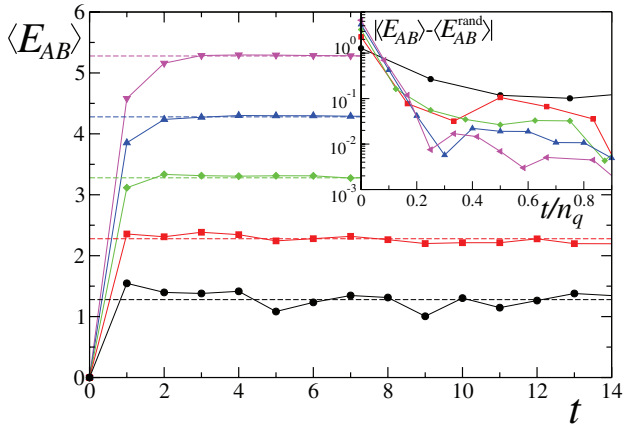

FIG. 1 (color online). Time evolution of the average bipartite entanglement of a quantum state, starting from a state of the computational basis (eigenstate of the momentum operator $\hat{n}$), and recursively applying the quantum sawtooth map (1) at $K = 1.5$ and, from bottom to top, $n_q = 4, 6, 8, 10, 12$. Dashed lines show the theoretical values of Eq. (2). Inset: convergence of $\langle E_{AB}\rangle(t)$ to the asymptotic value $\langle E_{AB}^{\mathrm{rand}}\rangle$.

As discussed above, multipartite entanglement should generally be described in terms of a function, rather than by a single number. We therefore show in Fig. 2 the probability density function $p(E_{AB})$ for the entanglement of all possible balanced bipartitions of the state $|\psi_{t=30}\rangle$. This function is sharply peaked around $\langle E_{AB}^{\mathrm{rand}}\rangle$, with a relative standard deviation $\sigma_{AB}/\langle E_{AB}\rangle$ that drops exponentially with n_q (see the inset of Fig. 2) and is very small (~ 0.1) already at $n_q = 4$. For this reason, we can conclude that multipartite entanglement is large and that it is reasonable to use the first moment $\langle E_{AB}\rangle$ of $p(E_{AB})$ for its characterization. We have also calculated the corresponding probability densities for random states (dashed curves in Fig. 2); their average values and variances are in agreement with the values obtained from states generated by the sawtooth map. The fact that for random states the distribution $p(E_{AB})$ is peaked around a mean value close to the maximum achievable value $E_{AB}^{\max} = n_q/2$ is a manifestation of the "concentration of measure" phenomenon in a multidimensional Hilbert space [5,6].

Stability of multipartite entanglement.—In order to assess the physical significance of the generated multipartite entanglement, it is crucial to study its stability when realistic noise is taken into account. Hereafter we model quantum noise by means of unitary noisy gates that result from an imperfect control of the quantum computer hardware [16]. We follow the noise model of Ref. [17]. One-qubit gates can be seen as rotations of the Bloch sphere about some fixed axis; we assume that unitary errors

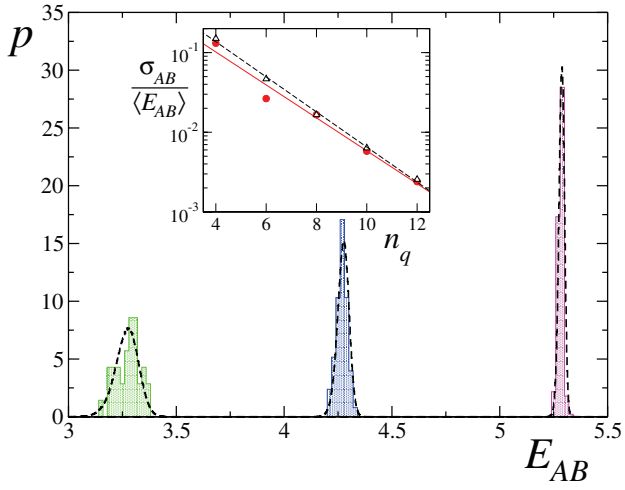

FIG. 2 (color online). Probability density function of the bipartite von Neumann entropy over all balanced bipartitions for the state $|\psi_t\rangle$, after 30 iterations of map (1) at $K = 1.5$. Various histograms are for different numbers of qubits: from left to right $n_q = 8, 10, 12$; dashed curves show the corresponding probabilities for random states. Inset: relative standard deviation $\sigma_{AB}/\langle E_{AB}\rangle$ as a function of n_q (full circles) and best exponential fit $\sigma_{AB}/\langle E_{AB}\rangle \sim e^{-0.48 n_q}$ (continuous line); data and best exponential fit $\sigma_{AB}/\langle E_{AB}\rangle \sim e^{-n_q/2}$ for random states are also shown (empty triangles, dashed line).

slightly tilt the direction of this axis by a random amount. Two-qubit controlled-phase shift gates are diagonal in the computational basis; we consider unitary perturbations by adding random small extra phases on all the computational basis states. Hereafter we assume that each noise parameter ε_i is randomly and uniformly distributed in the interval $[-\varepsilon, +\varepsilon]$; errors affecting different quantum gates are also supposed to be completely uncorrelated: every time we apply a noisy gate, noise parameters randomly fluctuate in the (fixed) interval $[-\varepsilon, +\varepsilon]$.

Starting from a given initial state $|\psi_0\rangle$, the quantum algorithm for simulating the sawtooth map in the presence of unitary noise gives an output state $|\psi_{\varepsilon_I,t}\rangle$ that differs from the ideal output $|\psi_t\rangle$. Here $\varepsilon_I = (\varepsilon_1, \varepsilon_2, \ldots, \varepsilon_{n_d})$ stands for all the n_d noise parameters ε_i that vary upon the specific noise configuration (n_d is proportional to the number of gates). Since we do not have any *a priori* knowledge of the particular values taken by the parameters ε_i, the expectation value of any observable A for our n_q-qubit system will be given by $\mathrm{Tr}[\rho_{\varepsilon,t}A]$, where the density matrix $\rho_{\varepsilon,t}$ is obtained after averaging over noise:

$$\rho_{\varepsilon,t} = \left(\frac{1}{2\varepsilon}\right)^{n_d} \int d\varepsilon_I |\psi_{\varepsilon_I,t}\rangle\langle\psi_{\varepsilon_I,t}|. \quad (3)$$

The integration over ε_I is estimated numerically by summing over $\mathcal{N}$ random realizations of noise, with a statistical error vanishing in the limit $\mathcal{N} \to \infty$. The mixed state ρ_ε may also arise as a consequence of nonunitary noise; in this case Eq. (3) can also be seen as an unraveling of ρ_ε into stochastically evolving pure states $|\psi_{\varepsilon_I}\rangle$, each evolution being known as a quantum trajectory [18].

We now focus on the entanglement content of $\rho_{\varepsilon,t}$. Unfortunately, for a generic mixed state of n_q qubits, a quantitative characterization of entanglement is not known, nor unambiguous [19]. Anyway, it is possible to give numerically accessible lower and upper bounds for the bipartite distillable entanglement $E_{AB}^{(D)}(\rho_\varepsilon)$:

$$\max\{S(\rho_{\varepsilon,A}) - S(\rho_\varepsilon), 0\} \le E_{AB}^{(D)}(\rho_\varepsilon) \le \log_2 \|\rho_\varepsilon^{T_B}\|, \quad (4)$$

where $\rho_{\varepsilon,A} = \mathrm{Tr}_B(\rho_\varepsilon)$ and $\|\rho_\varepsilon^{T_B}\| \equiv \mathrm{Tr}\sqrt{(\rho_\varepsilon^{T_B})^\dagger \rho_\varepsilon^{T_B}}$ denotes the trace norm of the partial transpose of ρ_ε with respect to party B.

In practice, we simulate the quantum algorithm for the quantum sawtooth map in the chaotic regime with noisy gates and evaluate the two bounds in Eq. (4) for the distillable entanglement of the mixed state $\rho_{\varepsilon,t}$, obtained after averaging over $\mathcal{N}$ noise realizations. A satisfactory convergence for the lower and the upper bounds is obtained after $\mathcal{N} \sim \sqrt{N}$ and $\mathcal{N} \sim N$ noise realizations, respectively. In Fig. 3, upper panels, we plot the first moment of the lower (E_m) and the upper (E_M) bound for the distillable entanglement as a function of the imperfection strength. The various curves are for different numbers n_q of qubits; $\mathcal{N}$ depends on n_q and is large enough to obtain negligible statistical errors (smaller than the size of the symbols). In the lower panels of Fig. 3 we show the relative standard deviation of the probability density function (over all balanced bipartitions) for the distillable entanglement. As for pure states, we notice an exponential drop with n_q; the distribution width slightly broadens when increasing imperfection strength ε. We can therefore conclude that an average value of the bipartite distillable entanglement close to the ideal case $\varepsilon = 0$ implies that multipartite entanglement is stable.

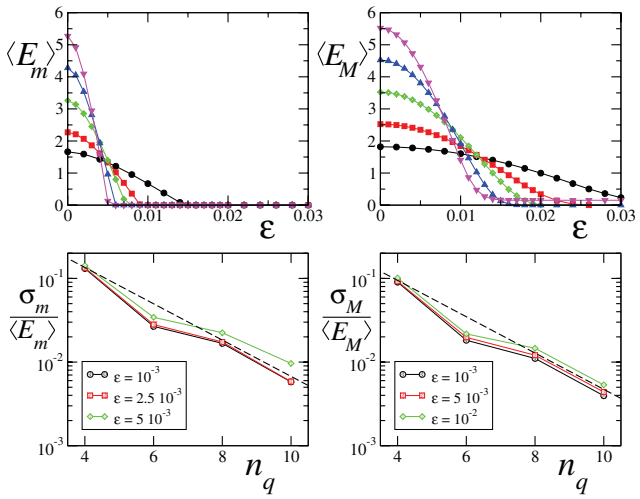

FIG. 3 (color online). Upper graphs: lower $\langle E_m\rangle$ (left panel) and upper bound $\langle E_M\rangle$ (right panel) for the distillable entanglement as a function of the noise strength at time $t = 30$. Various curves stand for different numbers of qubits: $n_q = 4$ (circles), 6 (squares), 8 (diamonds), 10 (triangles up), and 12 (triangles down). Lower graphs: relative standard deviation of the probability density function for distillable entanglement over all balanced bipartitions as a function of n_q, for different noise strengths ε. Dashed lines show a behavior $\sigma/\langle E\rangle \sim e^{-n_q/2}$ and are plotted as guidelines.

In order to quantify the robustness of multipartite entanglement with the system size, we define a perturbation strength threshold $\varepsilon^{(R)}$ at which the distillable entanglement bounds drop by a given fraction, for instance to 1/2, of their $\varepsilon = 0$ value, and analyze the behavior of $\varepsilon^{(R)}$ as a function of the number of qubits. Numerical results are plotted in Fig. 4; for both lower and upper bounds we obtain a power-law scaling close to

$$\varepsilon^{(R)} \sim 1/n_q. \quad (5)$$

It is possible to give a semianalytical proof of the scaling (5) for the lower bound measure, based on the quantum Fano inequality [20], which relates the entropy $S(\rho_\varepsilon)$ to the fidelity $F = \langle\psi_t|\rho_{\varepsilon,t}|\psi_t\rangle$: $S(\rho_\varepsilon) \lesssim h(F) + (1-F)\log_2(N^2-1)$, where $h(x) = -x\log_2(x) - (1-x)\log_2(1-x)$ is the binary Shannon entropy. Since $F \simeq e^{-\gamma\varepsilon^2 n_g t}$ [17,21], with $\gamma \sim 0.28$ and $n_g = 3n_q^2 + n_q$ being the number of gates required for each map step, we obtain, for $\varepsilon^2 n_g t \ll 1$,

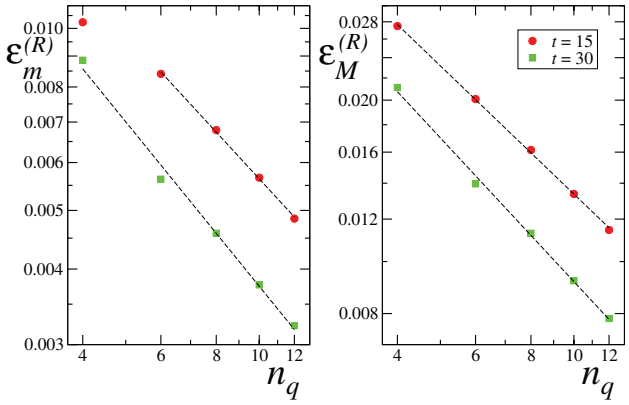

FIG. 4 (color online). Perturbation strength at which the bounds of multipartite entanglement halve (lower bound on the left panel, upper bound on the right panel), as a function of the number of qubits. Dashed lines are the best power-law fits of numerical data: $\varepsilon^{(R)} \sim n_q^{-0.79\pm0.01}$ at $t = 15$, $\varepsilon^{(R)} \sim n_q^{-0.9\pm0.01}$ at $t = 30$, for both lower and upper bounds.

$$S(\rho_\varepsilon) \leq \gamma\varepsilon^2 n_g t\left[-\log_2(\gamma\varepsilon^2 n_g t) + 2n_q + \frac{1}{\ln 2}\right]. \quad (6)$$

For sufficiently large systems the second term dominates (for $n_q = 12$ qubits, $t = 30$, and $\varepsilon \sim 5 \times 10^{-3}$, the other terms are suppressed by a factor $\sim 1/10$) and, to a first approximation, we can only retain it. On the other hand, an estimate of the reduced entropy $S(\rho_A)$ is given by the bipartite entropy (2) of a pure random state [4]. Therefore, from Eq. (4) we obtain the following expression for the lower bound of the distillable entanglement:

$$E_{AB}^{(D)}(\rho_\varepsilon) \geq \frac{n_q}{2} - \frac{1}{2\ln 2} - 6\gamma n_q^3 \varepsilon^2 t. \quad (7)$$

From the threshold definition $E_{AB}^{(D)}(\rho_{\varepsilon^{(R)}}) = \frac{1}{2}E_{AB}^{(D)}(\rho_0) = \frac{1}{2}S(\rho_A)$ we get the scaling (5) that is valid when $n_q \gg 1$: $\varepsilon_m^{(R)} \sim 1/\sqrt{24\gamma n_q^2 t}$. Notice that, for small systems as the ones that can be numerically simulated (see data in Fig. 4), the first term of Eq. (6) may introduce remarkable logarithmic deviations from the asymptotic power-law behavior. At any rate, the scaling derived from Eq. (7) is in good agreement with our numerical data, and also reproduces the prefactor in front of the power-law decay (5) up to a factor of 2.

Conclusions.—We have shown that quantum chaotic maps provide a convenient tool to efficiently generate in a robust way the large amount of multipartite entanglement close to that expected for truly random states. This result may become of practical relevance, since prototypes of quantum computers simulating these systems and, in particular, our specific model [22] have been already experimentally put on using a three-qubit NMR-based quantum processor [22,23]. The fact that distillable entanglement of balanced bipartitions remains almost maximal, up to a noise strength that drops only polynomially with the number of qubits, supports the possibility that multipartite entanglement of a large number of qubits might be used as a real physical resource in quantum information protocols.

We acknowledge support by MIUR-PRIN and EC-EUROSQIP. This work has been performed within the "Quantum Information" research program of Centro di Ricerca Matematica "Ennio de Giorgi" of Scuola Normale Superiore.

*Present address: International School for Advanced Studies (SISSA), Via Beirut 2-4, I-34014 Trieste, Italy.

[1] M. A. Nielsen and I. L. Chuang, *Quantum Computation and Quantum Information* (Cambridge University Press, Cambridge, 2000).
[2] G. Benenti, G. Casati, and G. Strini, *Principles of Quantum Computation and Information, Vol. I: Basic Concepts* (World Scientific, Singapore, 2004); *Principles of Quantum Computation and Information, Vol. II: Basic Tools and Special Topics* (World Scientific, Singapore, 2007).
[3] R. Jozsa and N. Linden, Proc. R. Soc. A **459**, 2011 (2003).
[4] D. N. Page, Phys. Rev. Lett. **71**, 1291 (1993).
[5] K. Życzkowski and H.-J. Sommers, J. Phys. A **34**, 7111 (2001).
[6] P. Hayden, D. W. Leung, and A. Winter, Commun. Math. Phys. **265**, 95 (2006).
[7] A. Harrow, P. Hayden, and D. Leung, Phys. Rev. Lett. **92**, 187901 (2004).
[8] C. H. Bennett *et al.*, IEEE Trans. Inf. Theory **51**, 56 (2005).
[9] P. Hayden *et al.*, Commun. Math. Phys. **250**, 371 (2004).
[10] J. Emerson *et al.*, Science **302**, 2098 (2003).
[11] Y. S. Weinstein and C. S. Hellberg, Phys. Rev. Lett. **95**, 030501 (2005).
[12] R. Oliveira, O. C. O. Dahlsten, and M. B. Plenio, Phys. Rev. Lett. **98**, 130502 (2007).
[13] A. J. Scott and C. M. Caves, J. Phys. A **36**, 9553 (2003).
[14] P. Facchi, G. Florio, and S. Pascazio, Phys. Rev. A **74**, 042331 (2006).
[15] G. Benenti *et al.*, Phys. Rev. Lett. **87**, 227901 (2001).
[16] A noisy gates model close to experimental implementations is discussed in J. I. Cirac and P. Zoller, Phys. Rev. Lett. **74**, 4091 (1995).
[17] D. Rossini, G. Benenti, and G. Casati, Phys. Rev. E **70**, 056216 (2004).
[18] T. A. Brun, Am. J. Phys. **70**, 719 (2002).
[19] M. B. Plenio and S. Virmani, Quantum Inf. Comput. **7**, 1 (2007).
[20] B. Schumacher, Phys. Rev. A **54**, 2614 (1996).
[21] S. Bettelli, Phys. Rev. A **69**, 042310 (2004).
[22] M. K. Henry *et al.*, Phys. Rev. A **74**, 062317 (2006).
[23] Y. S. Weinstein *et al.*, Phys. Rev. Lett. **89**, 157902 (2002).